Available online at www.sciencedirect.com

ScienceDirect

Ceramics International 40 (2014) 39–45

CERAMICS INTERNATIONAL

www.elsevier.com/locate/ceramint

Novel high dielectric constant and low-loss tetragonal tungsten bronze dielectrics $Ba_5LnMgNb_9O_{30}$ (Ln = La, Nd, Sm, Gd and Yb)

Xiaohong Wang[a,b], Mengxu Li[a,b], Chang Zhou[a,b,*], Mengjie Wang[a,b], Wenzhong Lu[a,b]

[a]School of Optical and Electronic Information, Huazhong University of Science and Technology, Wuhan 430074, China
[b]Key Lab of Functional Materials for Electronic Information (B), MOE, Huazhong University of Science and Technology, Wuhan 430074, China

Received 2 May 2013; received in revised form 15 May 2013; accepted 27 May 2013
Available online 5 June 2013

Abstract

Five novel dielectric ceramics $Ba_5LnMgNb_9O_{30}$ (Ln = La, Nd, Sm, Gd and Yb) were synthesized using a conventional solid-state reaction method. The phase structure, microstructure and dielectric properties of the prepared ceramics were investigated. Results show that the ceramics exhibit tetragonal tungsten bronze structure with fully occupied A-sites. Only tungsten bronze structure can be observed in the ceramics of which Ln refers to La, Nd, Sm and Gd, while tungsten bronze structure and $YbNbO_4$ were found in the ceramic of which Ln refers to Yb. All the ceramics exhibit high dielectric constant (ε_r = 272 ~ 429), with the ceramics of which Ln refers to La, Nd, Sm and Yb possessing low dielectric loss with the order of 10^{-3} at 1 MHz. By decreasing the rare-earth ionic radius, the transition temperature increases from −114 °C to 45 °C and then decreases to −58 °C, while the maximum dielectric constant increases to 460 at Ln = Sm and subsequently decreases. The phase transition is a diffuse phase transition (DPT) in the ceramics, while the diffuse exponent γ increases gradually as the ionic radius of rare earth element decreases from that of La^{3+} to that of Gd^{3+}, and decreases thereafter. The temperature coefficients of dielectric constant of the ceramics with Ln = La, Nd, Sm and Yb are −1229 ppm/°C, −1542 ppm/°C, −1171 ppm/°C and −1067 ppm/°C respectively in the range of 20–80 °C at 1 MHz.

Keywords: C. Dielectric properties; D. Niobates; E. Capacitors; Tungsten bronze structure

1. Introduction

Dielectrics with tetragonal tungsten-bronze (TB) structure have attracted much attention due to their unique structure and great promise in multiferroic [1], pyroelectric [2], piezoelectric [3], nonlinear optics [4] and high-frequency dielectric applications [5]. The TB structure in the general formula $(A_1)_2(A_2)_4(C)_4(B_1)_2(B_2)_8O_{30}$ consists of the corner-linked BO_6 and three types of channels (square A_1, pentagonal A_2 and triangle C) which are available for cations occupying. The flexibility of the TB framework can tolerate stuffed (A–C sites are fully occupied), filled (A sites are fully occupied) and unfilled (A sites are partially occupied) occupancy of the channels, allowing for precisely tuning their physical properties [6–8]. Generally, ceramics with a filled TB structure is more stable [9] than its counterparts and do not easily suffer from optical damage when exposed under certain power levels at room temperature [10]. Recent research shows that some ceramics with a filled TB structure possess high dielectric constant (ε_r), low dielectric loss (tan δ), which can satisfy the miniaturization requirement in electroceramics industry.

Sebastian and Chen et al. proposed some promising candidates to obtain high dielectric constant (ε_r = 100 ~ 175) dielectric ceramics with a filled TB structure in $BaO–Ln_2O_3–TiO_2–M_2O_5$ quaternary system (Ln = La, Sm, Nd; M = Ta, Nb) [11–16]. The ceramics possess low dielectric loss in the order of $10^{-3} \sim 10^{-4}$ and high temperature coefficient of dielectric constant (τ_ε) up to −741 ~ −2500 ppm/°C. Fang et al. studied $Ba_5LnZnNb_9O_{30}$ (Ln=La, Nd and Sm) ceramics, the values of τ_ε decreases and the ε_r of $Ba_5LaZnNb_9O_{30}$ is 310 [17]. $Ba_5LnZnTa_9O_{30}$ (Ln = La, Sm) system shows relative low τ_ε (< -1000 ppm/°C) and tan δ in the order of 10^{-3}, while ε_r is

*Corresponding author at: School of Optical and Electronic Information, Huazhong University of Science and Technology, No. 1037 Luoyu Road, Wuhan 430074, China. Tel.: +86 27 875 42594; fax: +86 27 875 43134.
E-mail address: rabbite6@126.com (C. Zhou).

0272-8842/$ - see front matter © 2013 Elsevier Ltd and Techna Group S.r.l. All rights reserved.
http://dx.doi.org/10.1016/j.ceramint.2013.05.100

less than 100 [18]. Previous work shows that ionic substitutions in the TB structure can play a critical role in tailoring the physical properties.

Since magnesium was observed to occupy the octahedral sites of niobium-based perovskites [19], considering the ionic radius of Mg^{2+} is approximate to Zn^{2+} and the Mg–O bond energy is stronger than Zn–O bond one, Mg tends to occupy the B-site in the TB structure and thus Mg-contained TB compounds may possess desired dielectric properties. The purpose of this study is to develop one kind of TB structure ceramic with high dielectric constant, low dielectric loss and relatively low temperature coefficient of dielectric constant. While very few work touches TB compounds in the BaO–Ln_2O_3–MgO–Nb_2O_5 system, this paper presents the structure and dielectric properties of TB compounds $Ba_5LnMgNb_9O_{30}$ (Ln=La, Nd, Sm, Gd, Yb). Meanwhile, the influence of various Ln ions at A-sites on dielectric properties and crystal structures are also discussed.

2. Experimental procedures

The ceramics with the nominal compositions of $Ba_5LnMgNb_9O_{30}$, abbreviated as BLMN, BNMN, BSMN, BGMN and BYMN for Ln=La, Nd, Sm, Gd and Yb respectively, were prepared with a conventional solid-state reaction approach. Commercial powders of reagent grade $BaCO_3$, Ln_2O_3, MgO and Nb_2O_5 were added to a ball mill jar in stoichiometric proportions and were milled for 4 h in ethanol with ZrO_2 media. After the slurry was dried, the powders were calcined at 1200 °C for 4 h. The calcined powders were milled and dried, then mixed with 5 wt% polyvinyl alcohol (PVA). The powders were dry pressed into disks at a pressure of 100 MPa in a 15 mm-diameter stainless steel cylindrical die. The disks were sintered at 1350 °C for 4 h in air. XRD measurements were performed using a Shimadzu XRD-7000 with Cu Kα radiation. The surface morphologies and compositions of the ceramics were determined using a scanning electron microscope (SEM, TESCAN Vega3, Czech) equipped with an energy dispersive X-ray (EDX) analyzer. The densities of the compacts were measured by Archimedes' method.

For electrical characterization, the ceramics samples were polished to disks with a thickness of about 1.0 mm. Silver pastes were painted on both sides of the samples. The samples were fired at 550 °C for 10 min. The dielectric response of the ceramic disks was measured using a precision impedance analyzer (WK6500B, Wanyne Kerr Electronics, UK) over the frequency range from 1 kHz to 5 MHz at temperature from −180 °C to +150 °C . The heating rate was fixed at 2 °C /min. For low temperature measurement between −180 °C and room temperature the sample was placed in a liquid nitrogen cryostat.

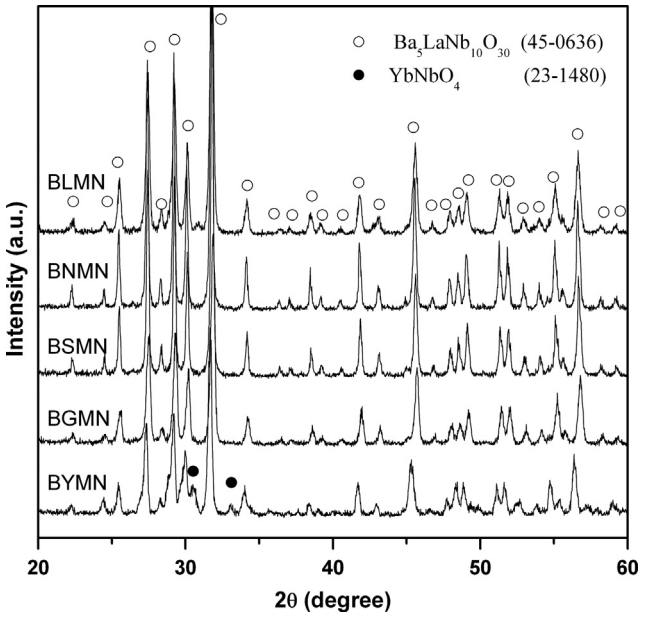

Fig. 1. X-ray diffraction patterns of $Ba_5LnMgNb_9O_{30}$ ceramics.

3. Results and discussion

All the samples were sintered into dense ceramics without any additive. The density of BLMN, BNMN and BSMN is in between 96.2% and 96.8% in theory for pore free materials, while the relative density of BYMN is 98.4%, and the relative density of BGMN is only 91.8%. The XRD patterns of the $Ba_5LnMgNb_9O_{30}$ ceramics with different rare-earth elements are shown in Fig. 1. All samples except BYMN are in pure tetragonal TB phase without detectable impurity phases. Both the primary tetragonal TB phase and the fergusonite $YbNbO_4$ are found to exist in BYMN. These observations suggest that the amount of rare earth can be accommodated in the TB framework is limited. The influence of Ln^{3+} ions on the tetragonal TB framework is demonstrated from the evolution

Table 1
The unit cell parameters, tolerance factor *t*, electronegativity difference *e* and stability factor *R* of $Ba_5LnMgNb_9O_{30}$.

Sample	*a* (Å)	*c* (Å)	*V* (Å^3)	*t*	*e*	*R*
BLMN	12.5939	3.9781	630.96	0.9903	2.116	1.1682
BNMN	12.5922	3.9801	631.11	0.9851	2.114	1.1663
BSMN	12.5733	3.9783	628.92	0.9834	2.112	1.1651
BGMN	12.5553	3.9731	626.3	0.9758	2.110	1.1623
BYMN	12.6399	3.9805	635.95	0.9720	2.107	1.1601

of the cell volume (Table 1). The ionic radius of lanthanides' ions is known to decrease with increasing atomic number. Thus the cell volume of the tetragonal TB matrix should decrease accordingly. This trend is observed when rare earth ions being changed from La to Gd, while the compound with Yb shows a different crystal chemical behaviors. The increment in cell volume of BYMN is probably associated with the Ba/Yb statistical distribution over both pentagonal and square channels. Thus the solution limitation of Ln^{3+} in BLnMN is probably associated with the distortion induced by the accommodation of the rare earth.

The stability of these TB structures can be evaluated by the tolerance factor proposed by Wakiya et al. [20]. For the general formula $(A_1)_2(A_2)_4(C)_4(B_1)_2(B_2)_8O_{30}$ for TB structure, there are two kinds of A sites for TB structure; A_1 and A_2 are 12- and 15-fold coordinated sites. Therefore, two kinds of tolerance factors for A-sites can be given by

$$t_{A1} = \frac{r_{A1} + r_O}{\sqrt{2}(r_B + r_O)} \quad (1)$$

$$t_{A2} = \frac{r_{A2} + r_O}{\sqrt{23-12\sqrt{3}}(r_B + r_O)} \quad (2)$$

where r_A, r_B and r_O are the ionic radii of the A- and B-site ions and O^{2-}, respectively. An average tolerance factor t is used to evaluate the relationship between tolerance and the stability of TB structure, which is defined as

$$t = \frac{t_{A1} + 2t_{A2}}{3} \quad (3)$$

Meanwhile, the average electronegativity difference e is another important parameter to measure the stability of the crystal structure, expressed as

$$e = \frac{(\chi_A - \chi_O) + (\chi_B - \chi_O)}{2} \quad (4)$$

where χ_A, χ_B and χ_O are the electronegativity of the A-, B-site ions and O^{2-}, respectively. So the average electronegativity difference e of $Ba_5LnMgNb_9O_{30}$ (Ln=La, Nd, Sm, Gd and Yb) can be calculated as

$$e = \frac{[5(\chi_{Ba} - \chi_O) + (\chi_{Ln} - \chi_O) + (\chi_{Mg} - \chi_O) + 9(\chi_{Nb} - \chi_O)]}{16} \quad (5)$$

As an evaluation to combinational effect of the tolerance and the electronegativity difference, R is defined as the stability factor, the larger the R, the more stable of the compound, given as

$$R = \frac{\sqrt{t^2 + e^2}}{2} \quad (6)$$

As shown in Table 2, the average tolerance factors and electronegativity differences of $Ba_5LnMgNb_9O_{30}$ were calculated using the revised effective ionic radii [21] and Pauling's electronegativity. With the radius of Ln^{3+} decreasing, both the tolerance factor and electronegativity difference decreases, resulting in the declination of the stability factor R. Observed from Table 1, the stability factor of BYMN is 1.1601. Therefore, BLMN, BNMN, BSMN and BGMN exhibit the stable TB structure without a secondary phase, while the secondary phase is observed in BYMN. So the minimum of R for the stabilization of $Ba_5LnMgNb_9O_{30}$ with TB structure is 1.16. Although it is difficult to precisely determine the coordination of cation ions, the course of the ionic radii suggests that Ba^{2+} predominately occupies the 15-fold coordinated A_2 sites, Ln^{3+} tends to occupy the 12-fold coordinated A_1 sites, and Nb^{5+} and Mg^{2+} occupy the 6-fold coordinated B sites. With the radius of Ln^{3+} decreasing, the stability of TB structure declines and the rare-earth element with small ionic radii may segregate and forms a secondary phase, which was confirmed in the XRD pattern of BYMN.

SEM micrographs of sintered ceramic surfaces are shown in Fig. 2. The microstructure indicates a monophasic constitution with uniformly packed rod-shaped grains in BNMN, BSMN and BGMN ceramics. It is clear that there are two types of grains in BYMN (Fig.2(d) and Table 2). The big rod-shaped grain (spot A) is specified as TB structure $Ba_6MgNb_9O_{30}$ with a little Yb. Small spherical grain (spot B) is identified as $YbNbO_4$. With the radius of Ln^{3+} decreasing, the grain sizes and the length of cylindrical grains increases. The preferred direction of grain growth of TB-structured materials is normally along the c-axis [22]. Such growth preference is supposed to be associated with the higher attachment energy on the c-plane, leading to a higher relative growth rate of the c-face [23]. As a result, the final grains elongate along the c-axis. An abnormal growth along the length direction is shown in Fig.2(d), the length of cylindrical grains is reach to 20 μm. It might be due to the lowering of the sintering temperature of the ceramics induced by rare-earth element. Previous studies have shown that dopants with low melting temperature will facilitate the grain growth of $Sr_xBa_{1-x}Nb_2O_6$ with TB structure, resulting in an abnormal grain growth [24]. Due to the cylindrical grain growth, more pores may be formed and thus the sample's relative density decreases. In this case, similar changes in the microstructure are observed. The pores are obvious in Fig. 2(b,c), but most pores are filled with small $YbNbO_4$ grains in Fig. 2(d). Therefore, the relative density of BGMN is the lowest while BYMN ceramic is the densest among BLnMN ceramics.

The room-temperature dielectric characteristics of the $Ba_5LnMgNb_9O_{30}$ ceramics are shown in Table 3. These ceramics have high dielectric constants ε_r of 272–429 and low dielectric loss of $\sim 10^{-3}$ at 1 MHz. The dielectric constant increases from 324.7 to 429.48 and then declines with the decreasing of Ln^{3+} ionic radius. The increase of ε_r may be because of the fact that the smaller Ln^{3+} ions at the square channels (A_1 sites) is, the stronger distortion of the tetragonal TB framework. The higher porosity causes the lower dielectric constant and maximum dielectric loss in BGMN. The appearance of fergusonite without ferroelectricity lowers ε_r of BYMN ceramic. In comparison with ε_r in the range 110–170 and τ_ε in the range $-1000 \sim -2400$ ppm/°C for $Ba_5LnTi_3Nb_7O_{30}$ (Ln=Nd, Sm) [15,16], the ε_r of $Ba_5LnMgNb_9O_{30}$ is much higher and τ_ε is smaller. Meanwhile, the dielectric constant of $Ba_5LnMgNb_9O_{30}$ is higher and dielectric loss is lower than those of $Ba_5LnZnNb_9O_{30}$ (Ln=La, Nd, Sm), while τ_ε is

similar [17]. However, the trends of ε_r and tan δ varied with the atomic number of Ln are opposite with those of $Ba_5LnZnNb_9O_{30}$ (Ln=La, Nd, Sm), in which the samples were sintered at various temperatures while all the samples in this study were sintered at 1350 °C .

Fig. 3(a–d) shows the temperature dependent dielectric spectra at various frequencies between −180 °C and 50 °C. There are only one significant broad dielectric peak at −114 °C, −70 °C, −48 °C, 45 °C and −58 °C (at 1 MHz) for BLMN, BNMN, BSMN, BGMN and BYMN, which suggests that only ferroelectric–paraelectric phase transitions from tetragonal 4mm symmetry to 4/mmm symmetry occurs and confirms that all compounds adopt the tetragonal TB structure. The positions of the maximum dielectric constant ε_{max} shift toward higher temperatures as the frequency increases. The appearance of the frequency dispersion is indicative of relaxor ferroelectric nature of ceramic solutions, which could arise from local compositional disorders in the A and B sites in TB structure. As there are five Ba atoms and one Ln atom for the six A_1 and A_2 positions, occupation of square channels (A_1 sites) by different cations creates disorder in the oxygen ion positions, due to the difference between Ba–O and Ln–O bonding lengths. Therefore, the disorder of ions in the unit cell should be the reason for the appearance of the frequency dispersion.

Table 2
The EDX data of the BYMN ceramics for spots A and B.

Elements	Atom (%)	
	Spot A	Spot B
O K	62.10	69.01
Mg K	2.09	–
Nb L	22.62	15.93
Ba L	12.81	–
Yb L	0.38	15.06

Fig. 4 shows the phase transition temperature (Curie temperature T_c) and the ε_{max} of $Ba_5LnMgNb_9O_{30}$ ceramics. The T_c at 1 MHz increases gradually from −114 °C to 45 °C by decreasing ion radius of Ln^{3+} and later decreases to −58 °C , where maximum dielectric constant ε_{max} has a similar trend with T_c and has a maximum value of 460 at Ln=Sm. The increase in T_c may be due to the distortion induced by the accommodation of the rare earth. When the smaller rare earth occupies square channels, the distortion of the TB framework

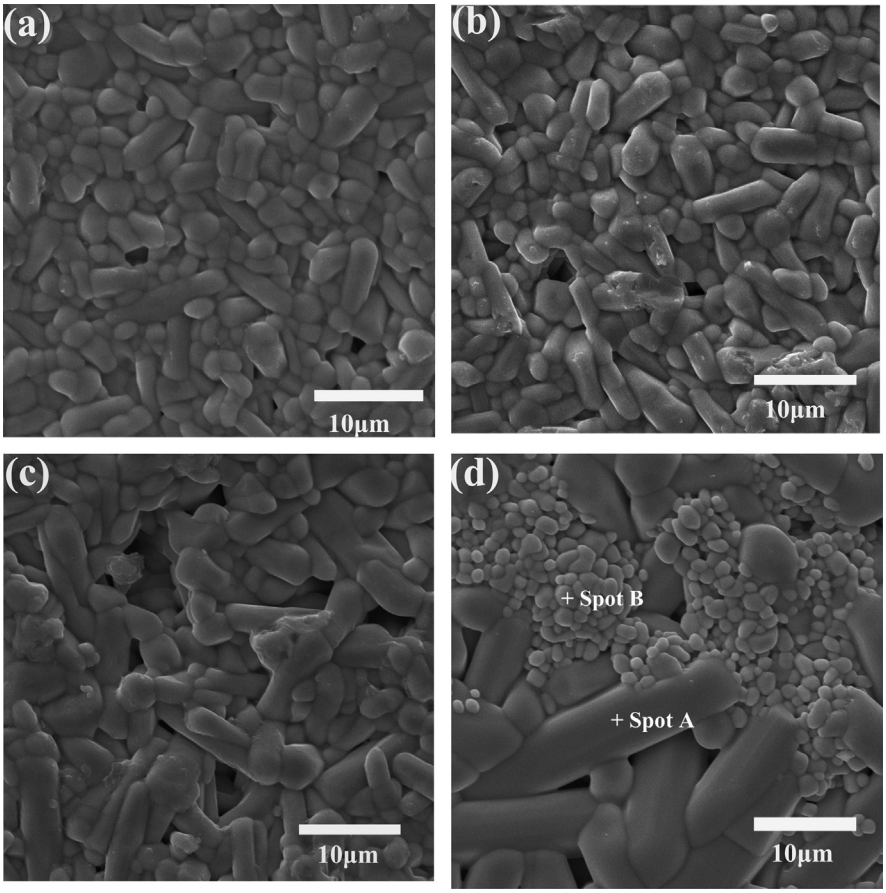

Fig. 2. SEM micrographs of $Ba_5LnMgNb_9O_{30}$ ceramics (a) BNMN, (b) BSMN, (c) BGMN, and (d) BYMN.

Table 3
Room temperature dielectric properties of $Ba_5LnMgNb_9O_{30}$ ceramics.

Samples	ε_r (1 MHz)	tan δ (1 MHz)	τ_ε (ppm/°C)
BLMN	324.70	0.0010	−1229
BNMN	386.88	0.0032	−1542
BSMN	429.48	0.0081	−1171
BGMN	335.30	0.0182	0.88%[a]
BYMN	272.03	0.0022	−1067

[a]It is the maximum permittivity change rate at 20–80 °C.

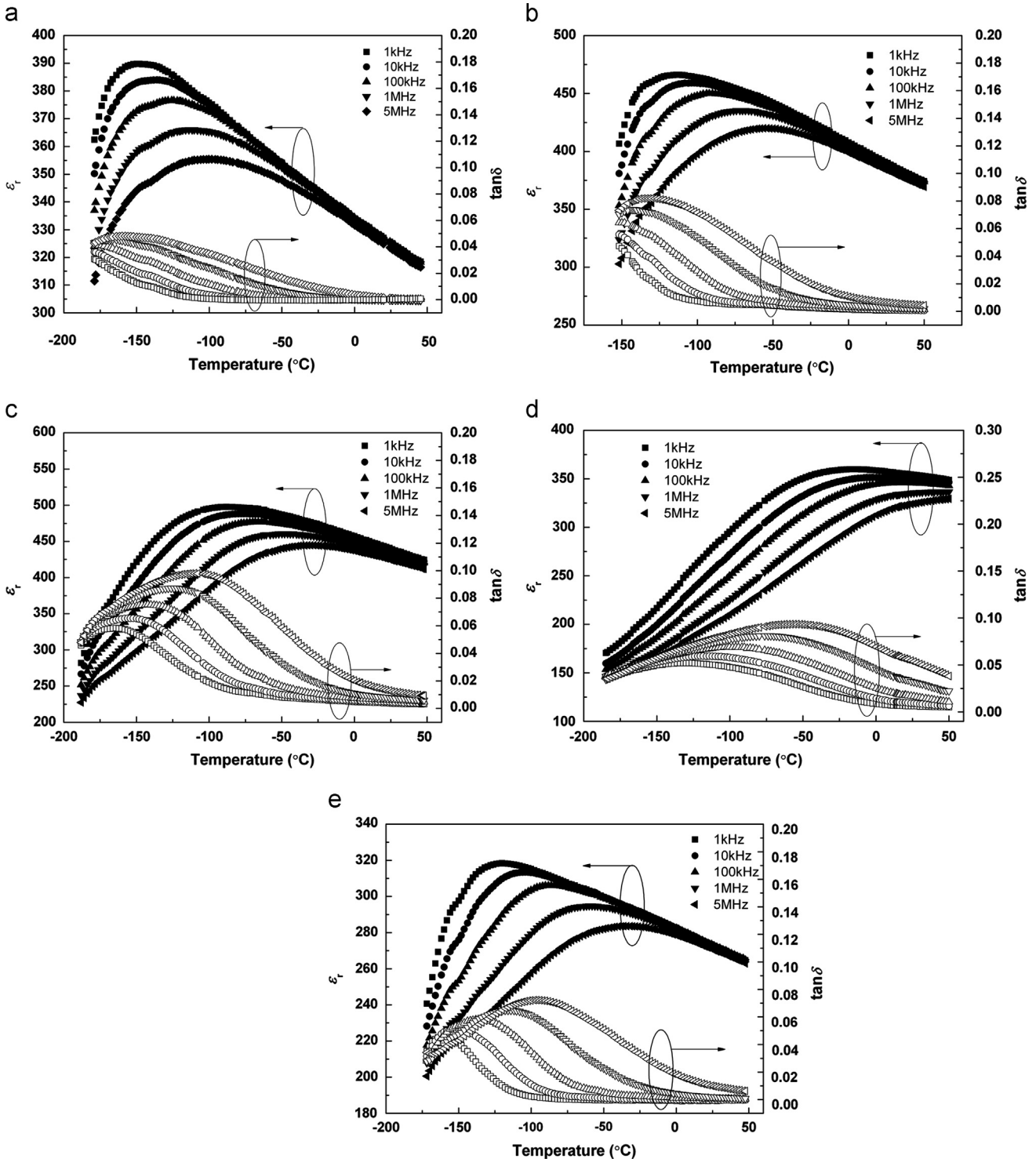

Fig. 3. Variation of ε_r and tan δ with temperature for the samples at different frequencies (a) BLMN, (b) BNMN, (c) BSMN, (d) BGMN and (e) BYMN.

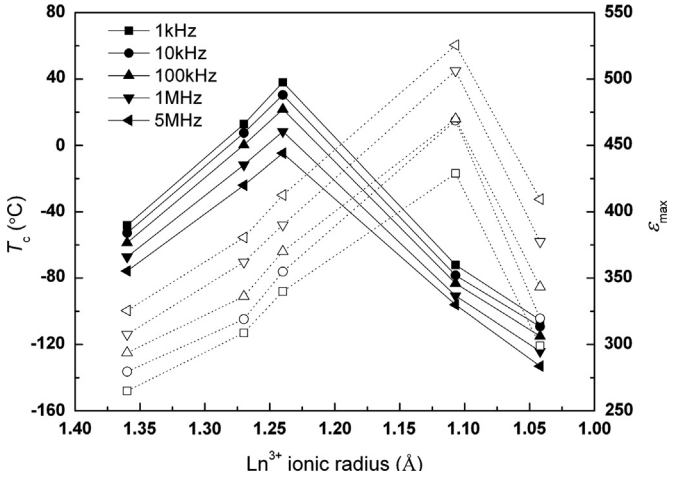

Fig. 4. ε_{max} (solid line) and T_c (dot line) of $Ba_5LnMgNb_9O_{30}$ ceramics as a function of ionic radius of Ln^{3+}.

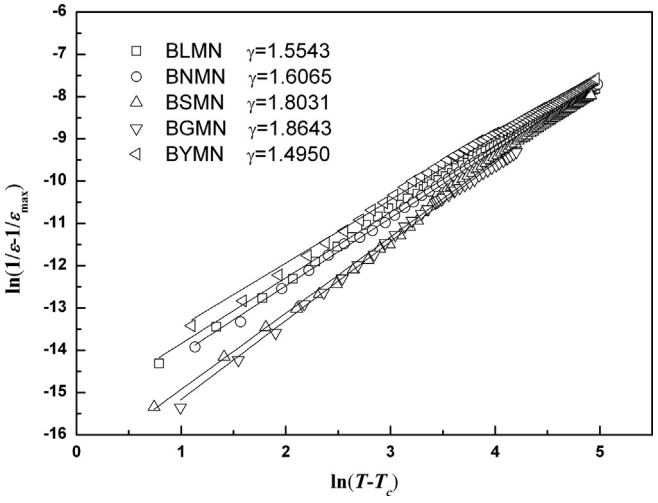

Fig. 5. Relationship between $\ln(1/\varepsilon-1/\varepsilon_{max})$ and $\ln(T-T_c)$ of $Ba_5LnMgNb_9O_{30}$ ceramics.

is stronger, leading to higher Curie temperature and higher maximum dielectric constant. In addition, the ionic character of the metal–oxygen bonds is weakened with the radius of Ln^{3+} decreasing, and subsequently the Curie temperature increases. The declination of ε_{max} at Ln=Gd may be due to the higher porosity of BGMN, which is 8.2%. When the radius of Ln^{3+} reduces to 1.04 Å (Ln=Yb), the fergusonite phase appears in BYMN ceramics, so the proportion of Ba/Yb in tetragonal TB structure is more than 5, it causes more Ba^{2+} ions to occupy A_1 sites, leading to less distortion of TTB framework and lower T_c and ε_{max}. Therefore, the T_c and ε_{max} increases gradually and later decreases with decreasing ionic radius of Ln^{3+}.

Shown in Fig.4, the broad dielectric peaks and T_c shifts to high temperature with an increasing frequency, it indicates that the phase transition is a diffuse phase transition (DPT). The DPT can be described by the modified Curie–Weiss law [25]

$$\frac{1}{\varepsilon}-\frac{1}{\varepsilon_{max}}=\frac{(T-T_c)^{\gamma}}{C} \quad (7)$$

where ε is the dielectric constant, T is the temperature, ε_{max} is the maximum dielectric constant at $T=T_c$, C is the modified Curie–Weiss constant and γ is a measurement of diffusivity. Fig. 5 shows the relationship between $\ln(1/\varepsilon-1/\varepsilon_{max})$ and $\ln(T-T_c)$ of the samples. The value of γ lies in between 1 (for normal or ideal ferroelectrics) and 2 (for completely disordered ferroelectrics) for all compounds, which confirms the diffused phase transition and the disordered state of ions in the structure. The diffuse exponent γ increases gradually from 1.5543 to 1.8643 by increasing atom number of rare-earth element and subsequently decreases to 1.4950 at Ln=Yb. This phenomenon shows the increase in disordering in the $Ba_5LnMgNb_9O_{30}$ system with decreasing ionic radius of the rare-earth element. The declination of γ in BYMN is due to the appearance of $YbNbO_4$, which can modify the composition of TB structure. The variation of the dielectric properties of $Ba_5LnMgNb_9O_{30}$ with the ionic radius of Ln^{3+} indicates that the accommodation of the rare earth in the TB framework is the critical parameter to determine the dielectric properties in this family of materials.

4. Conclusion

Five novel $Ba_5LnMgNb_9O_{30}$ (Ln=La, Nd, Sm, Gd and Yb) ceramics in the $BaO–Ln_2O_3–MgO–Nb_2O_5$ quaternary system were synthesized and characterized. Only a single phase with filled tetragonal TB structure is observed in $Ba_5LnMgNb_9O_{30}$ (Ln=La, Nd, Sm and Gd), while the TB structure and $YbNbO_4$ are existed in BYMN. With the declination of Ln^{3+} radium, the stability factor R decreases, leading to a further distortion induced by the accommodation of the rare earth. The present ceramics (Ln=La, Nd, Sm and Yb) are paraelectric phase at room temperature. The T_c increases gradually from −114 °C to 45 °C with decreasing ion radius of Ln^{3+} and later decreases to −58 °C , where ε_{max} has a similar trend with T_c. All the samples show a diffuse phase transition and the diffuse exponent γ increases gradually with the increasing atom number of the rare earth and subsequently decreases at Ln=Yb. All the present ceramics except BGMN indicated high ε_r (272–429) and low dielectric loss tan δ (in the order of 10^{-3} at 1 MHz). Meanwhile, the temperature coefficient of dielectric constant τ_ε varied from −1067 to −1542 ppm/°C in the temperature range of 20 °C–80 °C. These materials might have potential applications in temperature-compensating capacitors.

Acknowledgments

This work was supported by the Fundamental Research Funds for the Central Universities of China (2012QN153) and the Natural Science Foundation of Hubei Province (2010CDB02704).

References

[1] Y.J. Wu, S.P. Gu, Y.Q. Lin, Z.J. Hong, X.Q. Liu, X.M. Chen, Multiferroic ceramics in $BaO–Y_2O_3–Fe_2O_3–Nb_2O_5$ system, Ceramics International 36 (2010) 2415–2420.

[2] A. Glassam, Investigation of the electrical properties of $Sr_{1-x}Ba_xNb_2O_6$ with special reference to pyroelectric detection, Journal of Applied Physics 40 (1969) 4699–4712.

[3] R.J. Xie, Y. Akimune, K. Matsuo, T. Sugiyama, Dielectric and ferroelectric properties of tetragonal tungsten bronze $Sr_{2-x}Ca_xNaNb_5O_{15}$ ($x=0.05–0.35$) ceramics, Applied Physics Letters 80 (2002) 835–837.

[4] W.C. Liu, C.L. Mak, K.H. Wong, $Sr_{1.8}Ca_{0.2}NaNb_5O_{15}$ films for electro-optic modulator application, Journal of Physics D: Applied Physics 42 (2009) 105114.

[5] R. Ubic, I. Mreaney, W.E. Lee, Microwave dielectric solid–solution phase in system $BaO–Ln_2O_3–TiO_2$ (Ln=lanthanide cation), Journal of International Materials Reviews 43 (1998) 205–219.

[6] L.G. Van Uitert, H.J. Levinstein, J.J. Rubin, et al., Some characteristics of niobates having filled tetragonal tungsten bronze-like structures, Materials Research Bulletin 3 (1968) 47–58.

[7] D.C. Arnold, F.D. Morrison, B-cation effects in relaxor and ferroelectric tetragonal tungsten bronzes, Journal of Materials Chemistry 19 (2009) 6485–6488.

[8] R.R. Neurgaonkar, J.G. Nelson, J.R. Oliver, Ferroelectric properties of the tungsten bronze $M_6^{2+}M_2^{4+}Nb_8O_{30}$ solid solution systems, Materials Research Bulletin 27 (1992) 677–684.

[9] T. Ikeda, K. Uno, K. Oyamada, A. Sagara, J. Kato, S. Takano, H. Sato, Some solid solutions of the $A_5B_{10}O_{30}$- and $A_6B_{10}O_{30}$-type tungsten-bronze ferroelectrics, Japanese Journal of Applied Physics 17 (1978) 341–348.

[10] R.J. Xie, Y. Akimune, K. Matsuo, T. Sugiyama, Dielectric and ferroelectric properties of tetragonal tungsten bronze $Sr_{2-x}Ca_xNaNb_5O_{15}$ ($x=0.05–0.35$) ceramics, Applied Physics Letters 80 (2002) 835–837.

[11] P. Koshy, L.P. Kumari, M.T. Sebastian, Preparation, characterization and dielectric properties of $Ba_3Ln_3Ti_5Nb_5O_{30}$ (Ln=La, Nd) ceramics, Journal of Materials Science: Materials in Electronics 9 (1998) 43–45.

[12] X.M. Chen, J.S. Yang, Dielectric characteristics of ceramics in $BaO–Nd_2O_3–TiO_2–Ta_2O_5$ system, Journal of the European Ceramic Society 19 (1999) 139–142.

[13] X.M. Chen, Y.H. Sun, X.H. Zheng, High permittivity and low loss dielectric ceramics in the $BaO–La_2O_3–TiO_2–Ta_2O_5$ system, Journal of the European Ceramic Society 23 (2003) 1571–1575.

[14] X.M. Chen, Z.Y. Xu, J. Li, Dielectric ceramics in the $BaO–Sm_2O_3–TiO_2–Ta_2O_5$ quaternary system, Journal of Materials Research 15 (2000) 125–129.

[15] X.H. Zheng, X.M. Chen, Crystal structure and dielectric properties of ferroelectric ceramics in the $BaO–Sm_2O_3–TiO_2–Nb_2O_5$ system, Solid State Communications 125 (2003) 449–454.

[16] X.H. Zheng, X.M. Chen, Dielectric ceramics with tungsten-bronze structure in the $BaO–Nd_2O_3–TiO_2–Nb_2O_5$ system, Journal of Materials Research 17 (2002) 1664–1670.

[17] L. Fang, Q. Yu, C.Z. Hu, H. Zhang, High dielectric constant and low-loss dielectric ceramics of $Ba_5LnZnNb_9O_{30}$ (Ln=La, Nd, and Sm), Materials Letters 61 (2007) 4140–4143.

[18] L. Fang, H. Zhang, J.F. Yang, R.Z. Yuan, H.X. Liu, Preparation, characterization and dielectric properties of $Ba_5LnZnTa_9O_{30}$ (Ln=La, Sm) ceramics, Materials Research Bulletin 39 (2004) 677–682.

[19] F. Galasso, Structure, Properties and Preparation of Perovskite-type Compounds, Pergamon Press, New York, 1969.

[20] N. Wakiya, J.K. Wang, A. Saiki, K. Shinozaki, N. Mizutani, Synthesis and dielectric properties of $Ba_{1-x}R_{2x/3}Nb_2O_6$ (R: rare earth) with tetragonal tungsten bronze structure, Journal of the European Ceramic Society 19 (1999) 1071–1075.

[21] R.D. Shannon, Revised effective ionic radii and systematic studies of interatomic distances in halides and chalcogenides, Acta Crystallographica A32 (1976) 751–767.

[22] W.W. Chen, S. Kume, C. Duran, K. Watari, Preparation of single crystalline $Sr_{0.5}Ba_{0.5}Nb_2O_6$ particles, Journal of the European Ceramic Society 26 (2007) 647–653.

[23] P. Hartman, P. Bennema, The attachment energy as a habit controlling factor: I. theoretical considerations, Journal of Crystal Growth 49 (1980) 145–156.

[24] M.S. Kim, J.H. Lee, J.J. Kim, H.Y. Lrr, S.H. Cho, Origin of abnormal grain growth in tungsten bronze structured ferroelectric $Sr_xBa_{1-x}Nb_2O_6$ ceramics, Japanese Journal of Applied Physics 41 (2002) 7048–7052.

[25] S.M. Pilgrim, A.E. Sutherland, S.R. Winzer, Diffuseness as a useful parameter for relaxor ceramics, Journal of the American Ceramic Society 73 (1990) 3122–3125.